frontiers | Frontiers in Earth Science

TYPE Original Research
PUBLISHED 25 August 2023
DOI 10.3389/feart.2023.1228489

Physico-mechanical properties and shielding efficiency in relation to mineralogical and geochemical compositions of Um Had granitoid, Central Eastern Desert, Egypt

Mohammed A. Rashwan[1], El Saeed R. Lasheen[2]*, Wael Abdelwahab[1], Mokhles K. Azer[1], Hesham M. H. Zakaly[3,4,5]*, Saad S. Alarifi[6], Antoaneta Ene[7]* and Ismail A. Thabet[8]

[1]Geological Sciences Department, National Research Centre, Giza, Egypt, [2]Geology Department, Faculty of Science, Al-Azhar University, Cairo, Egypt, [3]Institute of Physics and Technology, Ural Federal University, Yekaterinburg, Russia, [4]Computer Engineering Department, Faculty of Engineering and Natural Sciences, Istinye University, Istanbul, Türkiye, [5]Physics Department, Faculty of Science, Al-Azhar University, Assiut, Egypt, [6]Department of Geology and Geophysics, College of Science, King Saud University, Riyadh, Saudi Arabia, [7]INPOLDE Research Center, Department of Chemistry, Physics and Environment, Faculty of Sciences and Environment, Dunarea de Jos University of Galati, Galati, Romania, [8]Geology Department, Faculty of Science, Tanta University, Tanta, Egypt

Check for updates

OPEN ACCESS

EDITED BY
Ahmed M. Eldosouky,
Suez University, Egypt

REVIEWED BY
David R. Lentz,
University of New Brunswick Fredericton, Canada
Saumitra Kumar Misra,
University of KwaZulu-Natal, South Africa

*CORRESPONDENCE
El Saeed R. Lasheen,
elsaeedlasheen@azhar.edu.eg
Hesham M. H. Zakaly,
h.m.zakaly@gmail.com
Antoaneta Ene,
antoaneta.ene@ugal.ro

RECEIVED 24 May 2023
ACCEPTED 10 August 2023
PUBLISHED 25 August 2023

CITATION
Rashwan MA, Lasheen ESR, Abdelwahab W, Azer MK, Zakaly HMH, Alarifi SS, Ene A and Thabet IA (2023), Physico-mechanical properties and shielding efficiency in relation to mineralogical and geochemical compositions of Um Had granitoid, Central Eastern Desert, Egypt. *Front. Earth Sci.* 11:1228489. doi: 10.3389/feart.2023.1228489

The current work aims to describe the physico-mechanical characteristics and shielding efficiency with reference to the mineralogical and geochemical compositions of the Neoproterozoic Um Had composite granitoid pluton in order to deduce their favorability as dimension stones. The Um Had granitoid pluton has an elliptical outline with a mean diameter of about 10 km. This pluton is a composite (ranging from white to reddish pink color), hard, massive, and medium- to coarse-grained granitoid body. It is classified as syenogranite according to their modal and bulk chemical compositions. Geochemically, the granitoid pluton is a highly calc-alkaline, peraluminous granite, formed by low degree partial melting of tonalitic source rock in a post-collisional tectonic setting. The physico-mechanical properties of the granitoid pluton under study satisfy the requirements of dimension stone in terms of their bulk density (from 2561 to 2564 kg/m^3), and to some extent water absorption capacity (from 0.38% to 0.55%). However, their compressive strength values (50.4–113.4 MPa) do not achieve the minimum requirement for interior use and light duty exterior use. This study delves into the potential of some of our syenogranite samples (I, IIA, IIS, and 10) as gamma radiation shielding materials. We have assessed the mass attenuation coefficient (G_{MAC}), effective atomic number (Z_{eff}), exposure build-up factor (EBF), and energy absorption build-up factor (EABF) for each of these samples. The G_{MAC} and Z_{eff} calculations were performed using the Phy-X online software, across a photon energy range of 0.015–15 MeV. Our findings suggest an inverse relationship between photon energy and $_{GMAC,}$ with the highest values observed for the (I) granite sample (~18). This study shows the promising radiation shielding capacity of our samples. The insights derived from G_{MAC}, Z_{eff}, EBF, and EABF can serve as a guide for the development of effective, naturally sourced radiation shielding materials.

KEYWORDS

Um Had granitoid, physical and mechanical properties, shielding efficiency, petrography, geochemistry

1 Introduction

Granitoid of variable sizes, shapes, chemical compositions, colors, and ages are abundant in south Sinai and the northern (in particular), central, and southern parts of the Egyptian Eastern Desert (e.g., Azer et al., 2020; Abdel-Karim et al., 2021; Lasheen et al., 2022a; Saleh et al., 2022a; Khaleal et al., 2023a; Khaleal et al., 2023b). They have grey, pink, and white (leucogranites) colors and range from calc alkaline (syn-collision) to alkaline (post-collision) as well as from metaluminous to strongly peraluminous in composition (Gharib, 2012; Abuamarah et al., 2022; Lasheen et al., 2022a). Notably, they are abundant, straddle about sixty percent of the total crystalline rocks in Egypt, and have high economic significance due to their high durability and aesthetic appearance (Alzahrani et al., 2022; Lasheen et al., 2023). Their distribution percent increases from the South to the North-Eastern Desert of Egypt (Stern and Hedge, 1985).

Recent studies show that some of these granitoids are rare-metal (Ta, Nb, Sn, Li, F, U, Th, and Zr), gemstone, and REE-bearing granitoid rocks (Khaleal et al., 2023a) and others can be utilized in the construction sector as decorative stones due to their high resistance and strength (Rashwan et al., 2019; 2023b; Alzahrani et al., 2022).

Worldwide, Egypt occupies the seventh place in the production of dimension stones (Mashaly et al., 2016), with a production volume of about 5.25 Million tons with 4% global sharing (Ericsson, 2019; Rashwan et al., 2023a). These rocks are widely used as decorative stones worldwide for construction of paving, flooring, cladding, and statues due to their great variety and high resistance and strength (Fort et al., 2013; Alzahrani et al., 2022; Rashwan et al., 2023a). Selected Igneous (granitoid of different types, basalt, gabbro, and ultramafic), metamorphic (marble and quartzite), and sedimentary (limestone) rocks represent the dominant natural industrial materials used as decorative stones in construction and building sectors (Gomes et al., 2020; Eroğlu and Çalik, 2023). Granitoid is a versatile natural material with a wide range of applications due to its excellent mechanical strength, durability, and radiation-shielding properties. With an impressive combination of high density, structural integrity, and low permeability, it offers excellent radiation protection and is often used in industries and facilities dealing with radioactive materials.

In the present work, we assess the ability of Um Had granitoid pluton for its use in the construction sector as a decorative stone. We reported new petrography and whole-rock chemical analyses (major oxides and trace elements) as well as mechanical and physical characteristics of Um Had granitoid. In addition, this study focuses on the utilization of the Um Had granitoid pluton as a radiation-shielding material. Granitoid, such as the one found in Um Had, possess unique geochemical characteristics that make them particularly suited to radiation-shielding applications.

2 Geologic setting

Egyptian Neoproterozoic rocks straddle the northern sector of the Arabian Nubian Shield (ANS), which represents the northern extension of the highly deformed Mozambique Belt. ANS makes up the eastern limb of the U-shaped Pan African Orogenic belt, one of the best examples of juvenile continental crust in the world (e.g., Lasheen et al., 2021; Khaleal et al., 2022a; Alharshan et al., 2022; Lasheen et al., 2022b; Hamdy et al., 2022; Kamar et al., 2022; Sami et al., 2023). The ANS encompasses both sides of the Red Sea: the Nubian Shield (western sector) and the Arabian Shield (Eastern sector) (e.g., Khaleal et al., 2022b; Saleh et al., 2022b; Sami et al., 2023).

The Um Had area lies in the Central Eastern Desert of Egypt, northwest to the intersection of Wadi Attala and Quseir—Qift asphaltic road (Figure 1A). Based on field observations, the main units exposed in the study area include gneiss, amphibolites, serpentinites, metavolcanics, ophiolitic mélange (metasediments), Hammamat metasedimentary rocks, Dokhan Volcanics, Attalla Felsite, and younger granitoid rocks (Figure 1B). Hammamat metasedimentary rocks (metaconglomerate, metagraywake, and metasiltstone) cover the greatest part of the study area, which are intruded by Attala felsite and the Um Had granitoid. The Um Had granitoid has a circular outline with a mean diameter of about 10 km. This pluton is hard, massive, and with a medium- to coarse-grained with buff, white to reddish pink in color (Figure 2A). It has an elevation point about 595 m above sea level. The southern part of the pluton has a sharp intrusive contact with Hammamat metasedimentary rocks, whereas the eastern part of the pluton lies against the Dokhan Volcanics. In addition, the Um Had granitoid is intruded by variable felsic (pegmatite and quartz), dikes, and veins. Some felsite and mafic xenoliths are recorded within the Um Had granitoid in the central and the northern parts. Some parts are intensively jointed in several trends, yielding small- to large-scale block weathering and exfoliation features (Figure 2B).

3 Materials and methods

Twenty-one samples were collected from the composite Um Had granitic pluton for our analyses. Twelve representative samples were examined in thin sections for the identification of preliminary mineral composition and textural relationships of rocks under investigation by using a polarizing microscope. The chemical (major oxides and trace elements) analyses of twelve samples were done using XRF (X-Ray Fluorescence technique) at the National Research Centre (NRC), Egypt. The samples were prepared as a bead with a 1 gm sample/10 gm flux ratio at 1150°C in an electroconductive furnace. ASTM E-1621 and ASTM D-7348 represent the dominant standard guides for analysis. The accuracy and precision of our analyses were better than ± 5% for major oxides and ±10% for trace elements.

The physical and mechanical characteristics of our studied samples were tested on cubic specimens of each Um Had granitoid sample (50 x 50 x 50 mm) (Figure 3). The water absorption, dry and wet bulk density, and apparent porosity were the main physical properties, which were measured

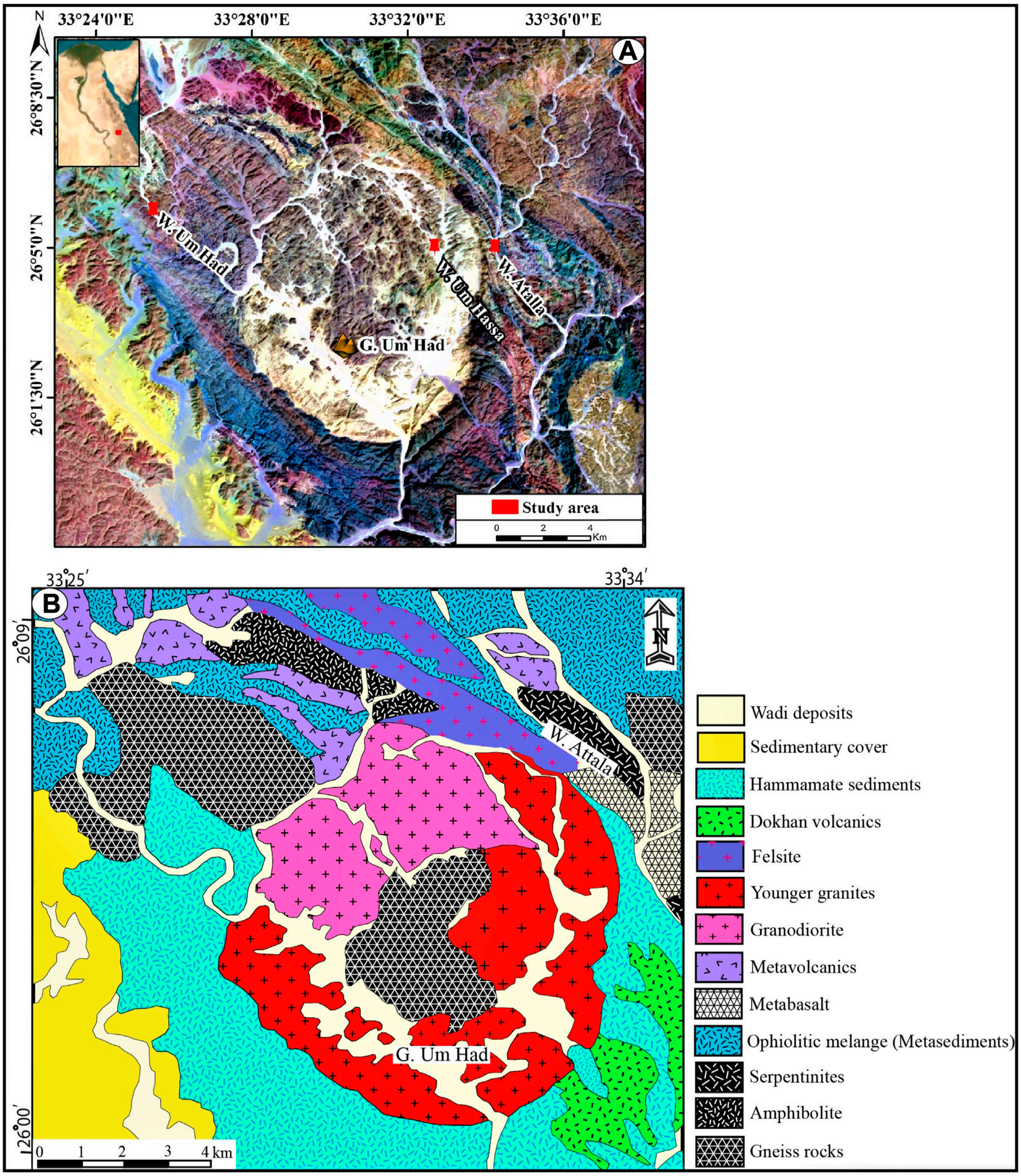

FIGURE 1
(A) Landsat image showing the location of Um Had area and **(B)** Geologic map of the area under investigation (Qaoud, 2014).

following the international standard specifications (ASTM C97/C97M, 2015; EN, 1936) based on Archimedes' method (Mosch and Siegesmund, 2007; Siegesmund and Snethlage, 2014; Rashwan et al., 2022; 2020). The mechanical tests including compressive strength with a rate of 0.5 MPa/s were also measured following the international standard specification (ASTM C170/C170M, 2015). The physical and mechanical tests were performed at the Marble and Granite Testing Laboratory (MGTL), National Research Centre, Egypt.

The examined samples were dried at 60°C until a constant mass was reached. Then, the weight was recorded to the nearest 0.01 gm. They were immersed in a tap water bath until complete saturation.

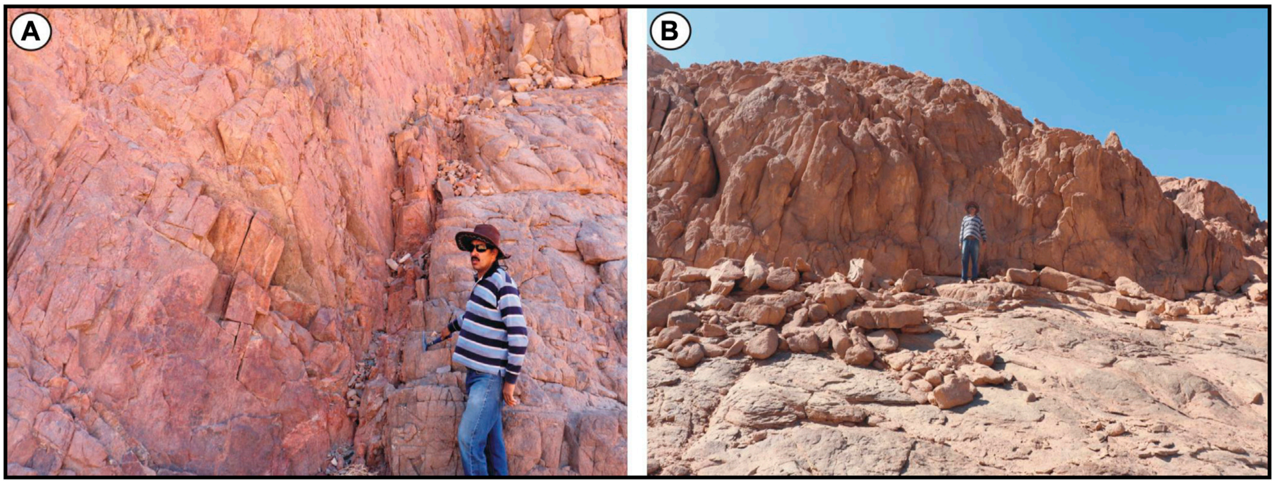

FIGURE 2
Field photographs exhibiting: **(A)** Variations in color of Um Had composite granitoid, and **(B)** Several joints, block weathering, and exfoliation features of Um Had granitoid. One of the authors is displayed for scale.

FIGURE 3
Cubic dimension of Um Had granitoid rocks for mechanical and physical tests.

The saturated samples were removed from the water bath, and the saturated-surface dry (SSD) weight was recorded to the nearest 0.01 gm. After that they were suspended in water and their suspended weight was then recorded to the nearest 0.01 gm. The physical properties were estimated through the following:

$$\text{Water absorption, \%} = 100 \times (\text{SSD weight} - \text{Dry weight})/\text{Dry weight} \quad (1)$$

$$\text{Apparent porosity, \%} = 100 \times (\text{SSD weight} - \text{Dry weight})/(\text{SSD weight}-\text{Suspended weight}) \quad (2)$$

$$\text{Dry Bulkdensity, kg}/m^3 = 1000 \times \text{Dry weight}/(\text{SSD weight}-\text{Suspended weight}) \quad (3)$$

$$\text{SSD Bulk density, kg}/m^3 = 1000 \times \text{SSD weight}/(\text{SSD weight}-\text{Suspended weight}) \quad (4)$$

A cubic specimen of each sample (50 × 50 × 50 mm) was prepared for the measurements of mechanical properties (compressive strength) following the requirements of the international standard test method (ASTM C170/C170M, 2015). According to this method, the investigated samples were completely dried at about 60°C. The loading area of the

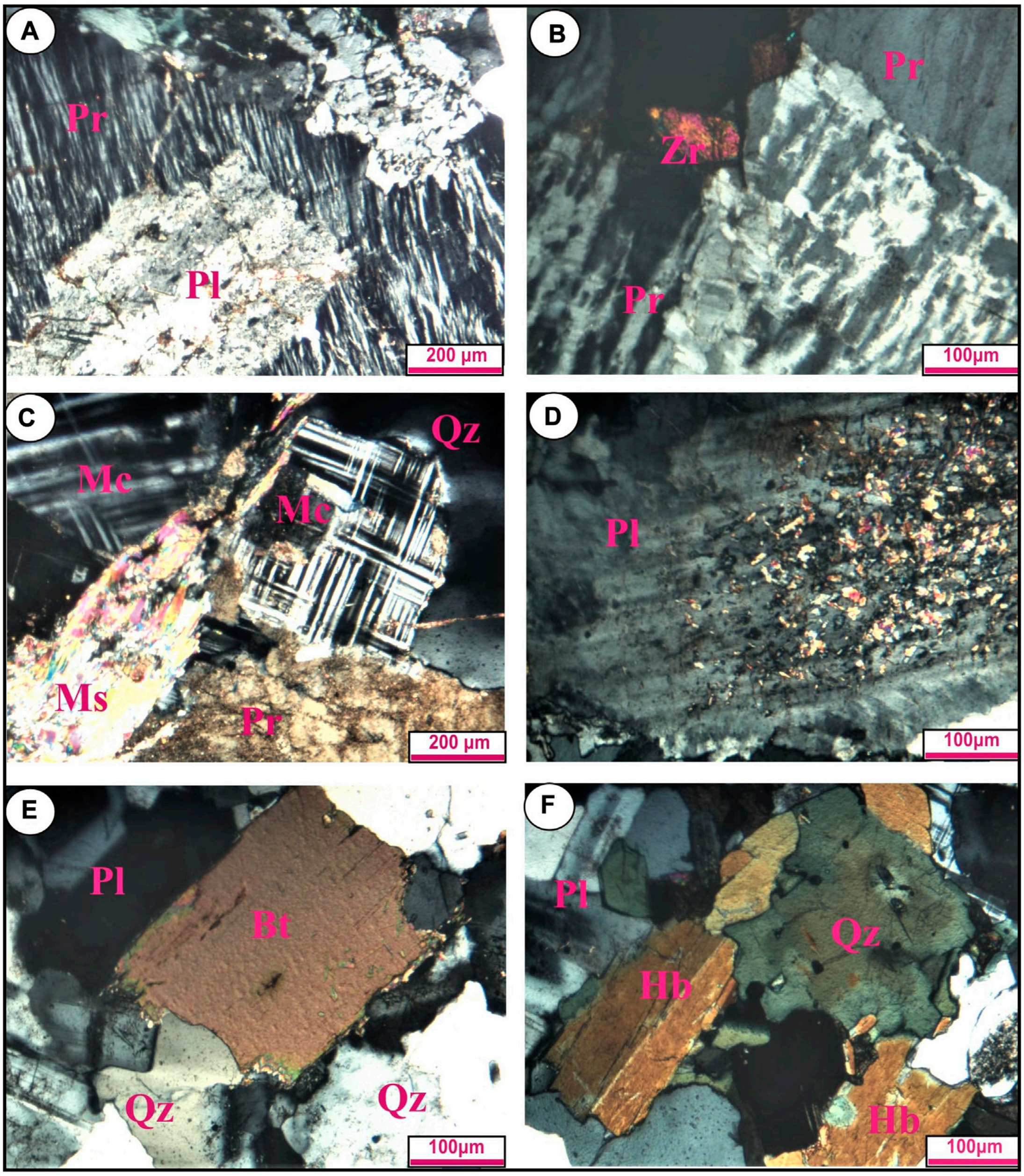

FIGURE 4
Photomicrographs exhibit: **(A)** Flamey orthoclase perthite (Pr) engulfing fine-grained plagioclase (Pl); **(B)** String orthoclase perthite enclosing euhedral zircon (Zr) crystal; **(C)** Pristine microcline (Mc) crystal associated with foliated muscovite (Ms) flakes; **(D)** Twisted plagioclase that reveals extensive saussurtization; **(E)** Partially chloritized biotite (Bt); and **(F)** Aggregated perfect carlsbad hornblende (Hb). Abbreviation of minerals after Whitney and Evans (2010).

samples were then calculated to the nearest 0.1 mm^2, after which the load was applied at a rate of 0.5 MPa/s using a compressive testing machine (SOILTEST Model: CT-6200-8) with a maximum capacity of 3,000 kN, until sample failure (Mashaly et al., 2018). The compressive strength was then calculated according to the equation:

$$\text{Compressive strength, MPa} = \text{Total load (N)}/\text{Loading area}\,(\text{mm}^2) \quad (5)$$

The mass attenuation coefficient (G_{MAC}) measured the probability of gamma ray or X-ray interaction per unit mass of a material and was therefore essential in assessing a material's potential for radiation shielding. The shielding parameters were computed using the platform Phy-X (Şakar et al., 2020).

4 Results and discussion

4.1 Petrographical investigation

On the basis of modal analysis, the examined Um Had composite granitoid with different colors were classified as syenogranites. They revealed a hypidiomorphic texture with

10.3389/feart.2023.1228489

TABLE 1 Bulk rock (major and trace elements) and normative minerals of the Um Had composite granitoid.

Oxides	I-1	I-2	I-3	Av.	IIA-1	IIA-2	IIA-3	Av.	IIS-1	IIS-2	IIS-3	Av.	10-1	10-2	10-3	Av.
SiO_2	72.72	72.61	72.24	72.52	73.46	73.61	73.75	73.61	73.83	73.68	73.88	73.80	71.58	71.68	71.94	71.73
TiO_2	0.32	0.31	0.34	0.32	0.20	0.27	0.24	0.23	0.20	0.16	0.14	0.17	0.18	0.19	0.18	0.19
Al_2O_3	13.44	13.10	13.15	13.23	13.09	13.10	13.13	13.11	13.02	13.01	13.03	13.02	15.06	15.15	14.98	15.06
Cr_2O_3	-	-	-	.	0.10	0.10	0.12	0.11	-	-	-	.	-	-	-	.
Fe_2O_3	3.40	3.46	3.45	3.44	2.65	2.08	2.70	2.48	2.25	2.17	2.42	2.28	1.89	2.05	1.94	1.96
Na_2O	3.42	3.56	3.56	3.51	3.59	3.53	3.21	3.44	4.10	3.99	3.89	3.99	4.30	4.20	3.95	4.15
K_2O	3.67	3.86	3.91	3.81	4.32	4.75	4.82	4.63	3.83	3.75	3.77	3.78	4.38	4.21	4.08	4.22
CaO	1.33	1.40	1.49	1.41	0.88	1.05	0.93	0.95	0.95	1.04	1.01	1.00	0.99	1.06	0.98	1.01
MgO	0.41	0.46	0.51	0.46	0.21	0.22	0.23	0.22	0.22	0.22	0.24	0.23	0.51	0.52	0.56	0.53
MnO	0.06	0.05	0.08	0.06	0.07	0.10	0.10	0.09	0.06	0.07	0.08	0.07	0.08	0.09	0.11	0.09
P_2O_5	0.21	0.26	0.21	0.23	0.08	0.06	0.06	0.07	0.11	0.09	0.09	0.10	0.13	0.12	0.12	0.12
LOI	0.43	0.43	0.43	0.43	0.37	0.37	0.37	0.37	1.17	1.17	1.17	1.17	0.45	0.45	0.45	0.45
Total	99.41	99.50	99.37	99.43	99.01	99.23	99.66	99.30	99.73	99.35	99.72	99.60	99.55	99.72	99.28	99.52
Normative values																
Q	35.92	34.20	33.22	34.45	34.08	32.50	34.47	33.69	33.28	33.83	34.57	33.89	27.30	28.45	30.79	28.84
C	1.93	1.14	0.86	1.31	1.10	0.38	1.09	0.86	0.67	0.71	0.93	0.77	1.76	2.04	2.58	2.13
Or	21.69	22.81	23.11	22.53	25.53	28.07	28.49	27.36	22.63	22.16	22.28	22.36	25.89	24.88	24.11	24.96
Ab	28.94	30.11	30.12	29.72	30.38	29.87	27.16	29.14	34.69	33.76	32.92	33.79	36.39	35.54	33.38	35.10
An	5.22	5.25	6.02	5.50	3.84	4.82	4.22	4.29	3.99	4.57	4.42	4.33	4.06	4.48	4.08	4.21
Hy	1.02	1.15	1.27	1.15	0.52	0.54	0.57	0.54	0.55	0.55	0.60	0.56	1.27	1.28	1.40	1.32
Il	0.14	0.11	0.16	0.14	0.16	0.21	0.21	0.19	0.12	0.14	0.17	0.14	0.16	0.19	0.24	0.20
Hm	3.40	3.46	3.45	3.44	2.65	2.08	2.70	2.48	2.25	2.17	2.42	2.28	1.89	2.05	1.94	1.96
Ru	0.25	0.25	0.26	0.25	0.11	0.16	0.13	0.13	0.13	0.09	0.05	0.09	0.10	0.09	0.05	0.08
Ap	0.50	0.61	0.50	0.54	0.19	0.14	0.14	0.16	0.26	0.21	0.21	0.23	0.31	0.28	0.28	0.29
Total	99.01	99.09	98.96	99.02	98.56	98.77	99.18	98.84	98.58	98.19	98.56	98.44	99.11	99.29	98.85	99.08

(Continued on following page)

10.3389/feart.2023.1228489

TABLE 1 (*Continued*) Bulk rock (major and trace elements) and normative minerals of the Um Had composite granitoid.

Oxides	I-1	I-2	I-3	Av.	IIA-1	IIA-2	IIA-3	Av.	IIS-1	IIS-2	IIS-3	Av.	10-1	10-2	10-3	Av.
Trace elements																
SC	2.90	2.70	2.99	2.86	4.50	4.60	4.33	4.48	7.50	7.34	7.56	7.47	3.90	3.86	4.07	3.94
V	8.60	8.40	8.75	8.58	1.90	1.78	1.89	1.86	2.70	2.68	2.79	2.72	7.30	7.27	7.35	7.31
Cr	24.80	24.43	24.86	24.70	36.60	36.21	36.71	36.51	9.10	9.08	9.37	9.18	2.80	2.75	2.81	2.79
Ni	2.80	2.71	2.83	2.78	0.50	0.42	0.41	0.44	1.30	1.08	1.36	1.25	3.80	3.81	3.79	3.80
Cu	4.70	4.60	4.81	4.70	4.00	3.74	3.98	3.91	4.80	4.76	4.81	4.79	3.90	3.95	3.89	3.91
Zn	64.30	64.22	64.43	64.32	50.20	50.11	49.43	49.91	61.60	61.46	61.58	61.55	80.70	80.69	79.88	80.42
Ga	18.90	18.88	18.99	18.92	18.90	18.83	19.00	18.91	22.20	22.04	22.29	22.18	20.90	20.85	20.32	20.69
Rb	52.10	52.33	52.43	52.29	68.40	68.22	68.27	68.30	84.00	83.89	83.68	83.86	130.00	130.72	129.57	130.10
Sr	177.50	177.69	177.11	177.43	80.60	80.32	80.71	80.54	93.20	93.13	93.27	93.20	165.60	165.47	165.37	165.48
Y	24.10	24.36	23.98	24.15	35.30	35.21	35.33	35.28	45.70	45.66	45.73	45.70	49.00	49.09	49.26	49.12
Zr	393.00	392.00	393.90	392.97	241.00	240.00	241.66	240.89	288.50	288.30	288.46	288.42	177.80	177.79	177.43	177.67
Nb	18.10	18.00	17.83	17.98	22.30	22.11	22.43	22.28	26.20	26.10	26.32	26.21	20.40	20.30	20.35	20.35
Cs	112.40	112.23	112.51	112.38	8.40	8.24	8.21	8.28	7.10	7.06	7.08	7.08	3.90	3.98	3.91	3.93
Ba	685.30	685.23	686.00	685.51	285.30	285.22	285.11	285.21	392.00	391.00	392.00	391.67	386.00	387.00	386.40	386.47
La	24.40	24.44	24.77	24.54	44.40	44.62	44.63	44.55	93.60	93.28	93.61	93.50	30.80	30.59	30.86	30.75
Ce	57.20	57.43	57.32	57.32	98.40	98.43	98.41	98.41	181.00	180.80	181.80	181.20	71.70	71.68	71.39	71.59
Nd	22.60	22.22	22.09	22.30	44.40	44.22	44.63	44.42	84.40	84.32	84.70	84.47	35.10	35.08	35.21	35.13
Pb	6.80	6.60	6.27	6.56	9.00	9.00	8.76	8.92	10.00	9.88	10.20	10.03	12.90	12.78	12.87	12.85
Th	7.10	7.00	6.80	6.97	12.90	12.46	12.85	12.74	15.30	15.22	15.51	15.34	17.50	17.49	17.43	17.47
U	0.40	0.32	0.29	0.34	1.30	1.10	1.32	1.24	0.40	0.37	0.33	0.37	1.40	1.36	1.42	1.39
R1	2677.40	2575.70	2537.94	2597.02	2536.43	2479.79	2571.47	2529.23	2504.48	2555.13	2593.51	2551.04	2164.57	2242.14	2383.49	2263.40
R2	426.28	429.58	442.68	432.85	361.02	379.93	368.47	369.81	367.96	377.39	375.52	373.62	426.64	436.15	426.49	429.76
Na_2O/K_2O	0.93	0.92	0.91	0.92	0.83	0.74	0.67	0.75	1.07	1.06	1.03	1.06	0.98	1.00	0.97	0.98
K_2O/Na_2O	1.07	1.09	1.10	1.09	1.20	1.35	1.50	1.35	0.93	0.94	0.97	0.95	1.02	1.00	1.03	1.02
Na_2O+K_2O	7.09	7.42	7.47	7.33	7.91	8.28	8.03	8.07	7.93	7.74	7.66	7.78	8.68	8.41	8.03	8.37
Agpaitic Index	0.71	0.77	0.77	0.75	0.81	0.84	0.80	0.81	0.84	0.82	0.80	0.82	0.79	0.76	0.73	0.76

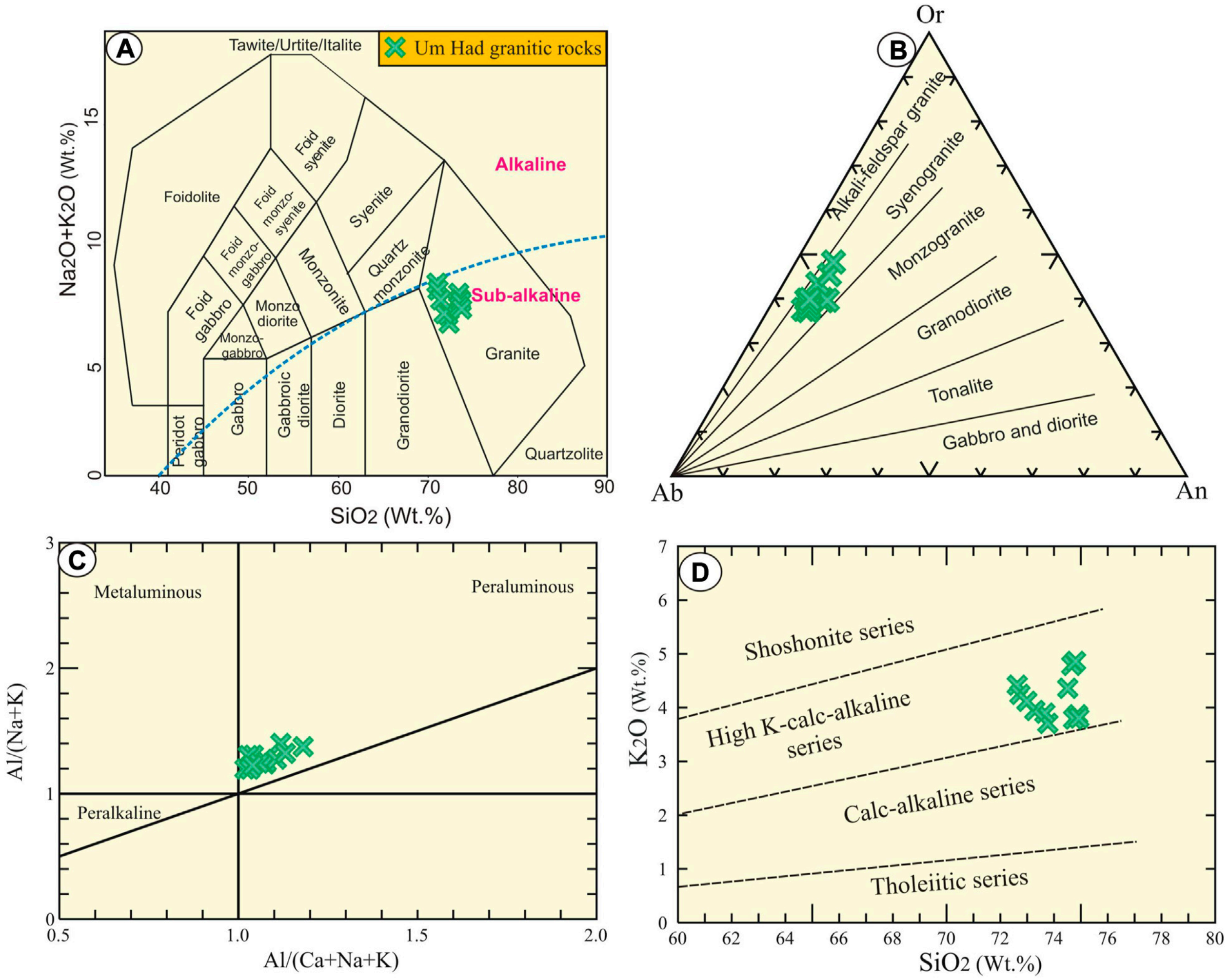

FIGURE 5
Bulk rock geochemistry of Um Had granitoid rocks: **(A)** SiO_2 (wt.%) vs. Na_2O+K_2O (wt.%) diagram (Middlemost, 1994); **(B)** Ab-Or-An diagram (Streckeisen, 1976); **(C)** Al/(Ca+Na+K) vs. Al/(Na+K) diagram (Shand, 1951); and **(D)** SiO_2 (wt.%) vs. K_2O (wt.%) diagram of (Rickwood, 1989).

medium- to coarse-grained crystals. Quartz, K-feldspars, plagioclase$_{(An4\text{-}13)}$, and muscovite were the dominant minerals with minor biotite, hornblende, and muscovite. Kaolinite, sericite, and epidote were the predominant secondary minerals, while iron oxides and zircon represented the main accessories. Quartz (22%-32%) occurred as anhedral crystals, revealing wavy extinction and sometimes present as small interstitial crystals. The dominant mineral was K-feldspar (microcline and orthoclase perthite) at 35%-42%. Perthite presented as flamey and string types (Figures 4A, B) with a clear to dusty surface and subhedral to anhedral crystals (Figure 4C). Occasionally, some fine-grained albitic plagioclase were enclosed in microcline megacryst (Figure 4A). Locally, they formed a micrographic texture due to intergrowths with quartz. Albite of medium- to coarse-graine ranged from 8% to 20%. In some samples, the albite exhibited a weak to strong saussurtization effect (Figure 4D). Biotite occurred as the main mafic mineral as fine flakes in the different granites. It was partially altered to chlorite along its periphery (Figure 4E). Minor hornblende occurred as fine-grained crystals with a clear set of two cleavages at an angle of ~120° (Figure 4F). Zircon was the main accessory mineral, which presented as very fine crystals commonly enclosed in microcline (Figure 4B).

4.2 Bulk rock geochemistry

The examined samples collected from the Um Had granitoid exhibit marginal variations in their chemical composition and normative values (Table 1). They have SiO_2 (71.58%–73.88%; av. 72.91%), Na_2O+K_2O (7.09–8.68; av. 7.88%), Al_2O_3 (13.01%–15.15%; av. 13.6%), and Fe_2O_3 (1.89–3.46; av. 2.53%), and minor concentrations (<1%) of TiO_2, MnO, MgO, Cr_2O_3, and P_2O_5. In addition, they possess $K_2O/Na_2O > 1$ (av. 1.1) in mean reflecting potassic nature. The main normative values are quartz (av. 32.72%), albite (av. 31.90%), and orthoclase (av. 24.31%). The Um Had granitoid are classified using variable discrimination diagrams. They are subalkaline in nature (after Middlemost, 1994) (Figure 5A). In addition, the examined rocks are classified as syenogranites based on their Ab, Or, and An

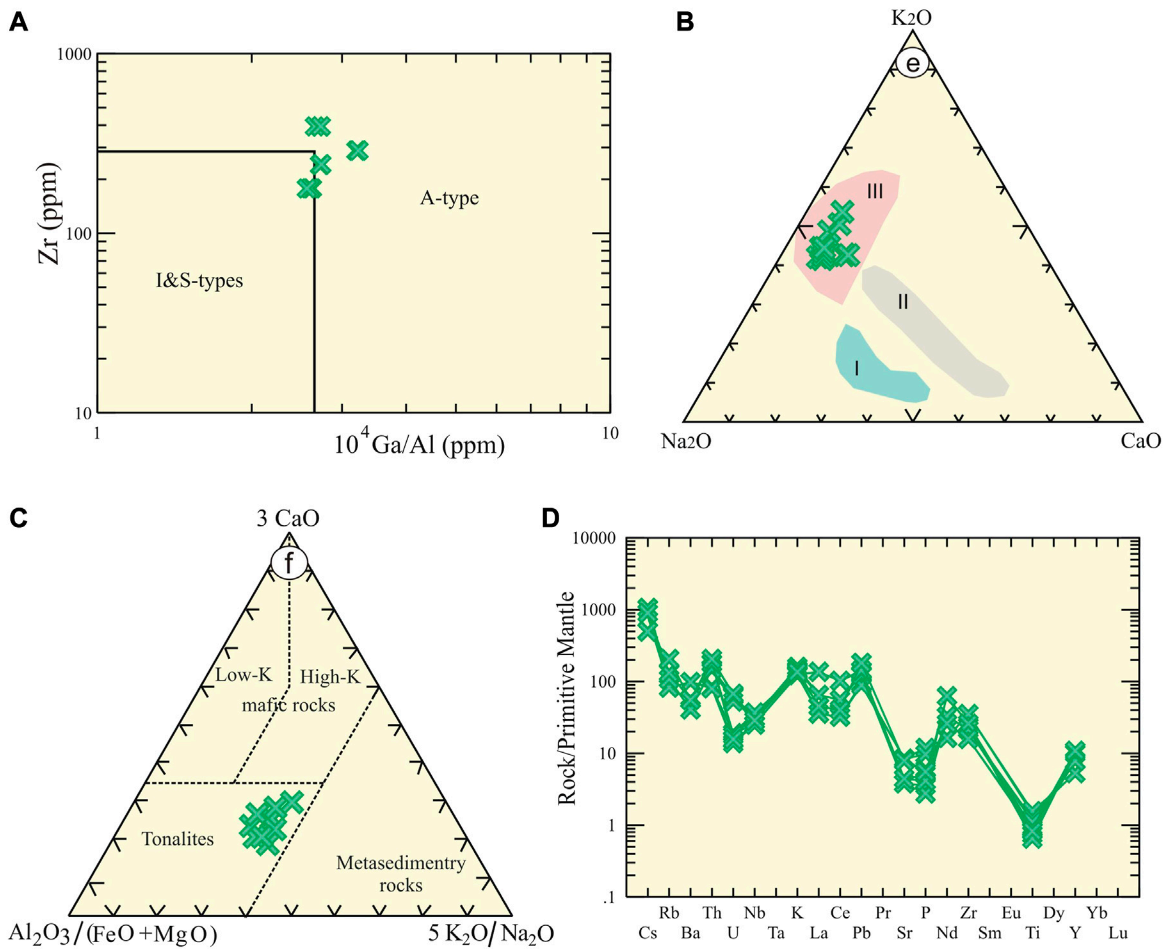

FIGURE 6
Bulk rock geochemistry of Um Had granitoid rocks: **(A)** 10^4 Ga/Al- Zr (ppm) (Whalen et al., 1987); **(B)** Na_2O-K_2O-CaO (wt.%) (Hassan and Hashad, 1990), I = granodiotite and metagabbro, II = early subphase of younger granites, and III = late phase of younger granites; **(C)** Al_2O_3/(FeO+MgO)-3 CaO-5 K_2O/Na_2O (wt.%) (Laurent et al., 2014), and **(D)** Spider diagram normalized to primitive mantle (Sun and McDonough, 1989).

normative values (after Streckeisen, 1976), (Figure 5B). Notably, these rocks have a peraluminous nature on the basis of their A/CNK (av. 1.51) (after Maniar and Piccoli, 1989) (Figure 5C). The studied rocks are high calc alkaline, with their agpaitic index ranging from 0.71 to 0.84 (<0.87). This is indicated by the SiO_2-K_2O binary diagram after Rickwood (1989) (Figure 5D).

The studied granitoid samples match well with A-type granitoid, as indicated by the Ga/Al versus Zr binary diagram after Whalen et al. (1987) (Figure 6A). The investigated granitoid rocks are of calc-alkaline in composition and of late to post-collisional type (III field) (Figure 6B) (after Hassan and Hashad, 1990). Um Had granitoid source can be inferred by some geochemical diagrams (after Laurent et al., 2014). They can by developed by the low partial melting degree of crustal tonalitic rocks (after Laurent et al., 2014), (Figure 6C). On the other hand, the distribution of trace elements was normalized to primitive mantle (after Sun and McDonough, 1989) of the studied Um Had granitoid rocks, as shown in Figure 6D. It is obvious from this pattern that the spider diagram shows positive anomalies of Cs, Rb, and Pb, and pronounced Ba, Sr, and Ti negative anomalies.

4.3 Physical and mechanical tests

Natural rocks used for decorative purposes in the interior (indoor) and exterior (outdoor) should undergo some physical and mechanical evaluations. The studied granitoid were tested for water absorption, bulk density, apparent porosity, and compressive strength. The main physico-mechanical properties of the studied granitoid are given in Supplementary Table S1 and illustrated in (Figures 7, 8 and Figure 9). The water absorption results (Figure 7A) ranged from 0.38% to 0.55%. The minimum value was recorded in granite (sample no. 10) with an average value of 0.41%, which corresponded with their porosity (Figure 7B) with an average value of 1.05%. On the other hand, the maximum water absorption value was recorded in granite (sample no. I) with

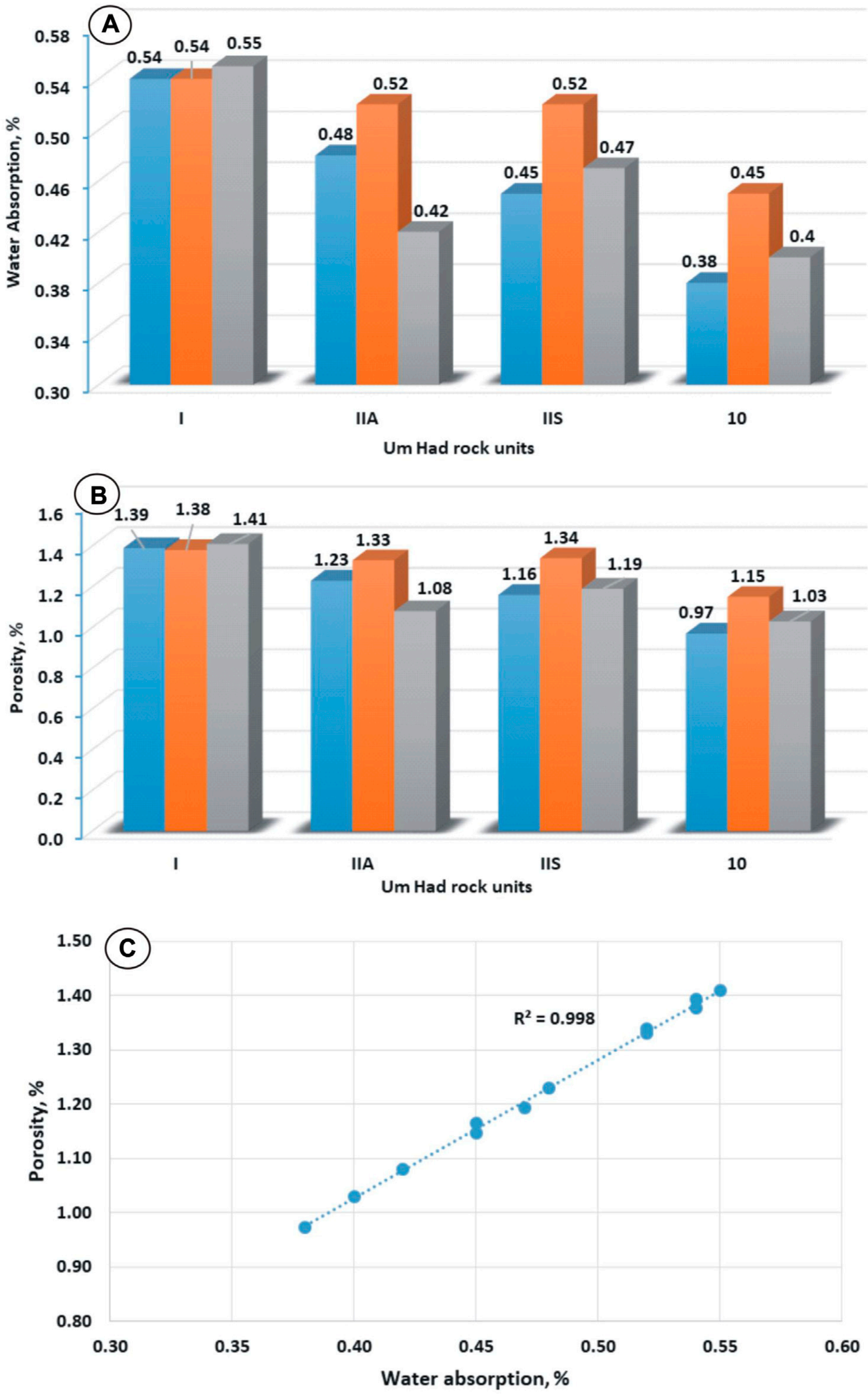

FIGURE 7
Physical properties of Um Had granitoid rocks: **(A)** water absorption, **(B)** porosity, and **(C)** water absorption vs. porosity relationships.

an average value of 0.54% that matches their average porosity value (1.39%). These values indicate that the water absorption increases with increasing apparent porosity, exhibiting a significant positive correlation coefficient (r = 1), as shown in (Figure 7C).

The dry and wet bulk densities of the granitoid rocks, as illustrated in Figures 8A, B, revealed that the granite sample (no. 10) recorded the maximum dry bulk density with average values of 2564.03 kg/m^3 and the minimum apparent porosity. On the other hand, the minimum bulk densities were achieved in the

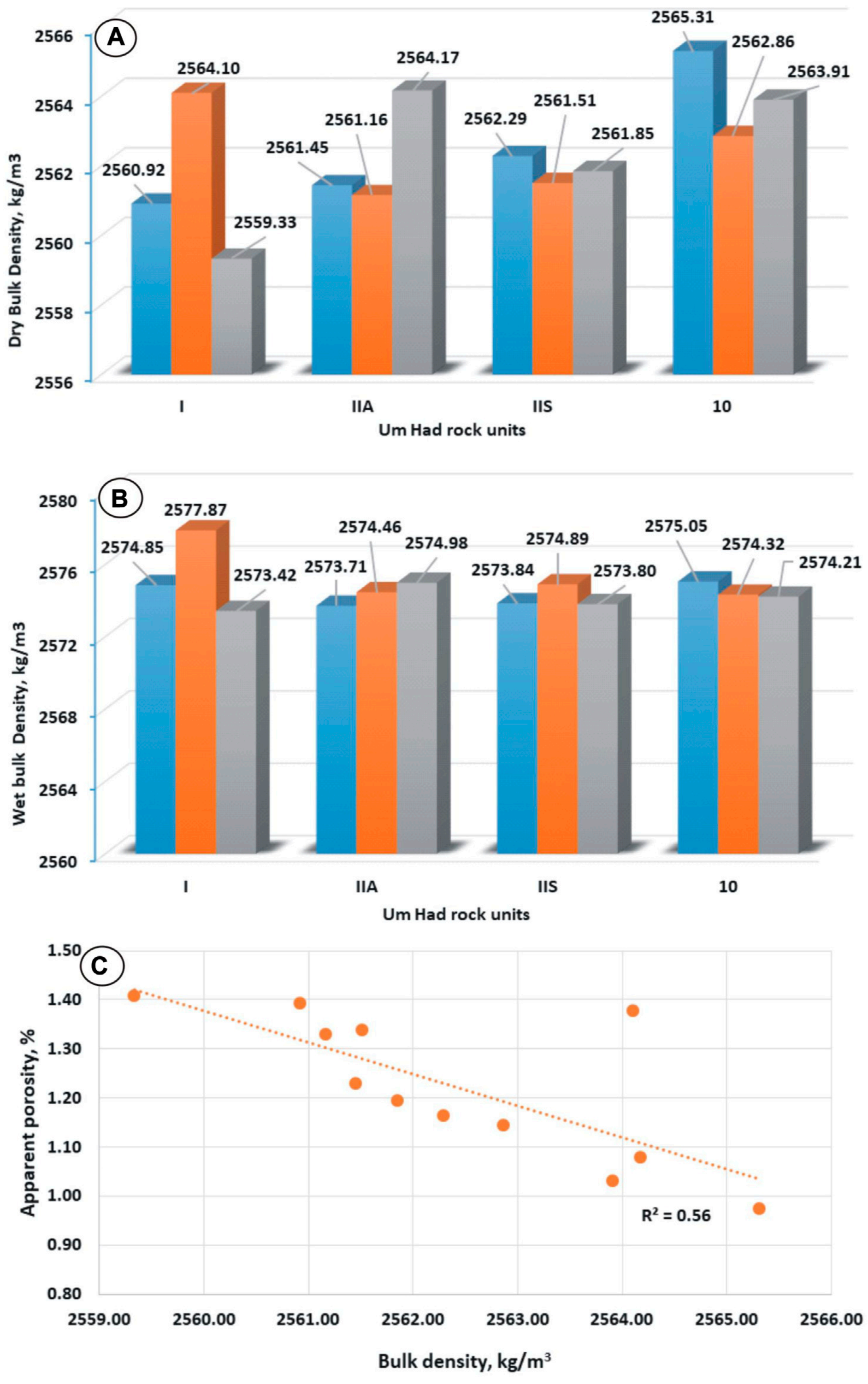

FIGURE 8
Physical properties of Um Had granitoid rocks: **(A)** dry bulk density, **(B)** wet bulk density, and **(C)** bulk density vs. apparent porosity relationship.

granitoid (no. I) with average values of 2561.45 kg/m^3 with the maximum apparent porosities. These results exhibit a relationship between the bulk density and apparent porosity (Figure 8C) with a significant negative correlation coefficient (r = −0.74).

Regarding the compressive strength results of the studied granites, there is a notable variation in the compressive strength values as shown in Figure 9. This figure shows that the granitoid rock sample of a minimum average normative quartz content (28.84%) and maximum average normative albite content

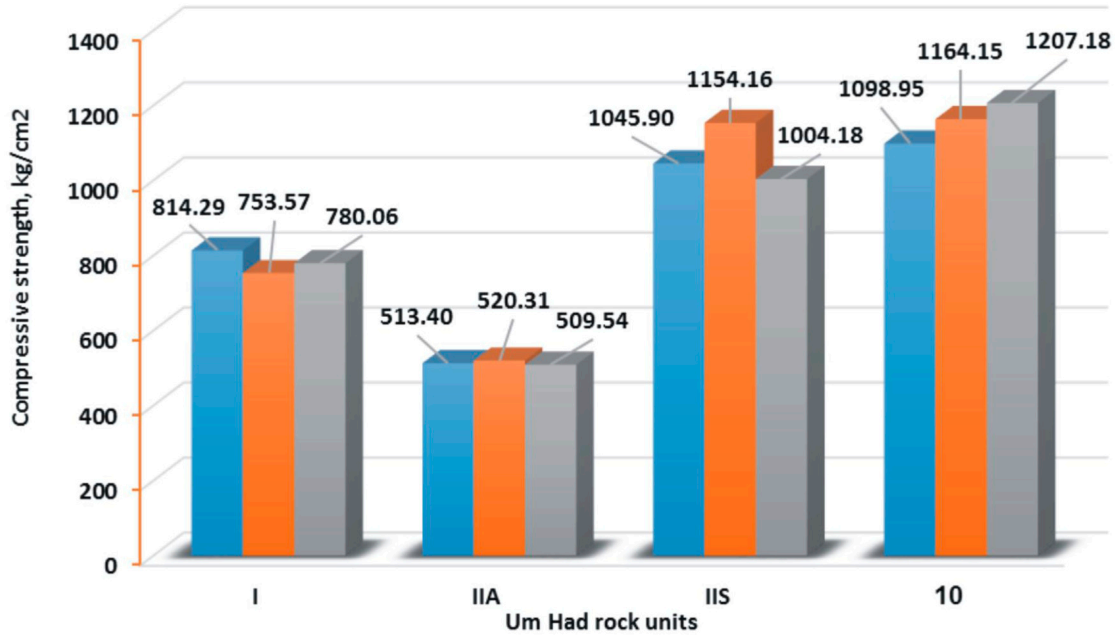

FIGURE 9
Mechanical properties (compressive strength) of UmHad granitoid.

(35.1%) (Table 1) records high strength values ranging from 1098.95 kg/cm^2 to 1207.18 kg/cm^2 with an average value of 1156.76 kg/cm^2. On the contrary, the lowest strength with an average value of 514.42 kg/cm^2 is recorded in the granitoid rock sample of a lowest average normative albite content (29.13%) and a highest average normative orthoclase content (27.36%) (Table 1). As mentioned above, the variations in the physical and mechanical strength may be attributed to the variations in the mineralogical composition of the studied granitoid rock samples as shown in Figures 10A–C. A negative variation in water absorption values with the total normative feldspar content (Figure 10A) with a correlation coefficient of $r = -0.67$ was observed, while a positive variation with normative hematite content (Figure 10B) with a correlation coefficient of $r = 0.77$ was also seen. Moreover, a positive variation in compressive strength values with the normative albite content (Figure 10C) with a correlation coefficient of $r = 0.85$ was also observed.

Comparing the results of the physical and mechanical data of the studied granites with the standard specification limits of the granite dimension stones (ASTM C615), it is found that all studied samples comply with the requirements of bulk density of a minimum limit (2560 kg/m^3). The determination of density is an important parameter for evaluating the compactness of rocks and consequently its hardness and resistance to abrasion. Regarding the water absorption results, the average value of the studied granitoid rock samples is 0.48%, which is slightly higher than the maximum specification limit (0.40%) and considered insignificant in countries with arid conditions. Although the compressive strength data of the studied granite does not achieve the minimum requirement of the same specification (131 MPa), making them suitable for exterior and heavy duty uses such as paving and landscape, these rocks could be acceptable for interior use and the light-duty purposes of exterior use as facades and cladding.

4.4 Radiation shielding

This research showed that among the examined Um Had granitoid, I, IIA, IIS, and 10, sample I exhibit the highest G_{MAC} values at 2.108 (at 15 keV), implying that this granite sample may offer superior radiation-shielding capabilities (Madbouly et al., 2022). However, it is important to consider that G_{MAC} decreases as the photon energy increases due to multiple types of photon-matter interactions, including the photoelectric effect, Compton scattering, and pair creation (Figure 11). This implies that while sample I exhibits superior shielding at lower photon energies, its performance may diminish with higher energy gamma rays. Moreover, another significant parameter in radiation shielding is the effective atomic number (Z_{eff}). This quantity gives insights into a material's capability to block incoming photons; a higher Z_{eff} suggests better shielding efficiency (sample I). For the examined granitoid, Z_{eff} reached its peak value at 15 MeV, with sample (I) having the highest Z_{eff} at 10.76 (Figure 12). This further indicates that the Um Had granite pluton (sample I) can offer better gamma radiation shielding than the other natural samples. In this investigation, we utilized the Geometry

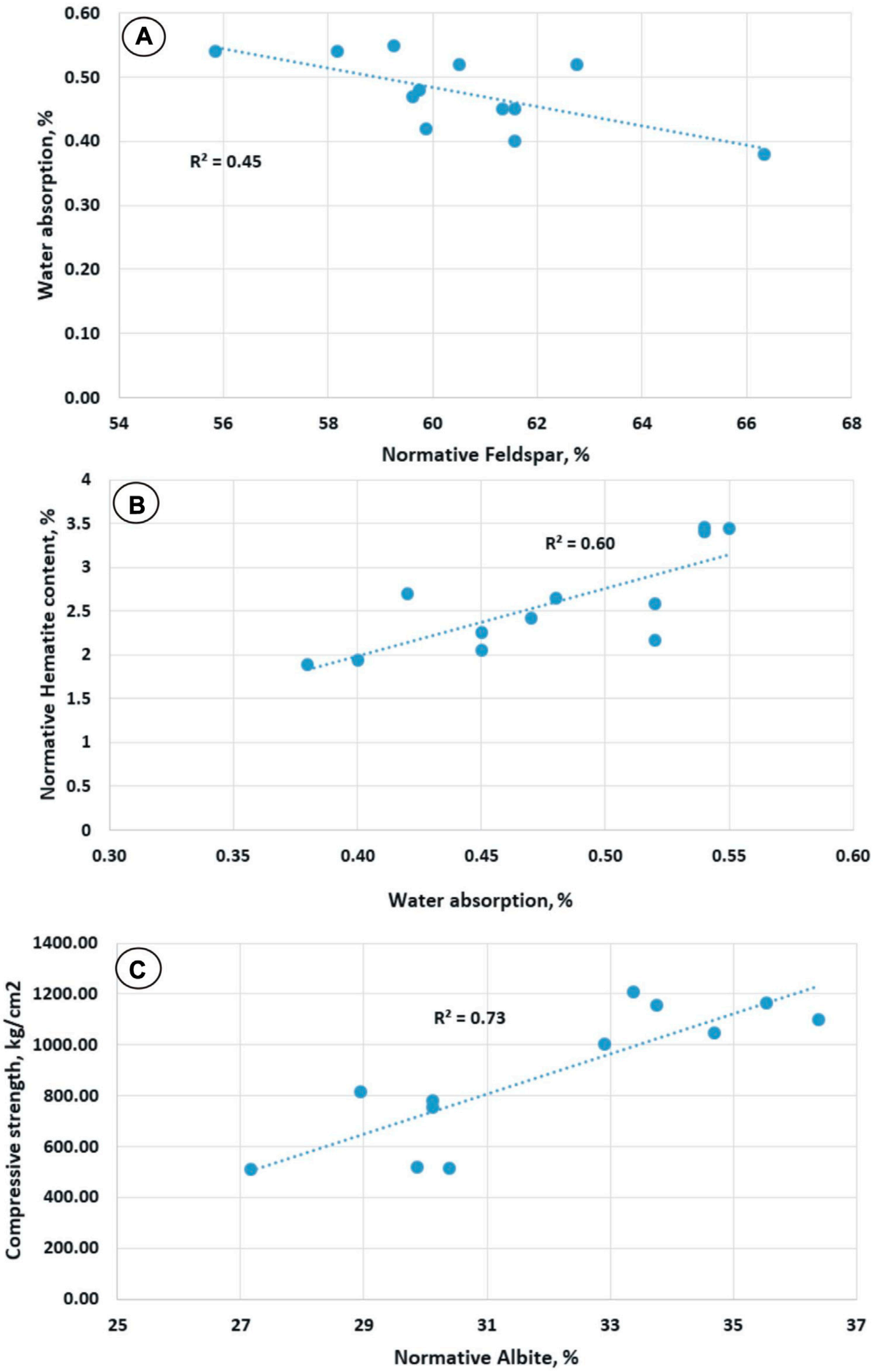

FIGURE 10
Relationship between physical properties of the Um Had granitoid and their mineralogical composition: **(A)** normative feldspar vs. water absorption and apparent porosity; **(B)** normative hematite vs. water absorption, and **(C)** normative albite vs. compressive strength.

Progressive (G-P) approach to calculate these factors for the granitic samples (I, IIA, IIS, and 10) (Singh and Badiger, 2014). This method, elaborated upon in a previous publication, enabled us to map out the correlation between the energy of the incoming photons and the variation in the EBF and EABF for these rock samples. The results (Figure 13; Supplementary

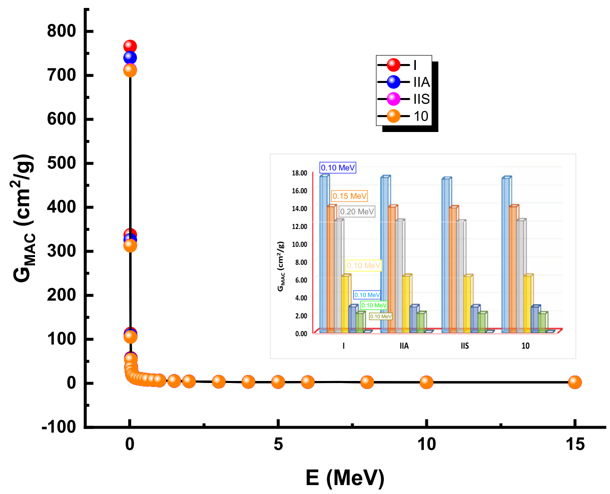

FIGURE 11
Depiction of the fluctuation in the mass attenuation coefficient relative to photon energy for the Um Had granitoid.

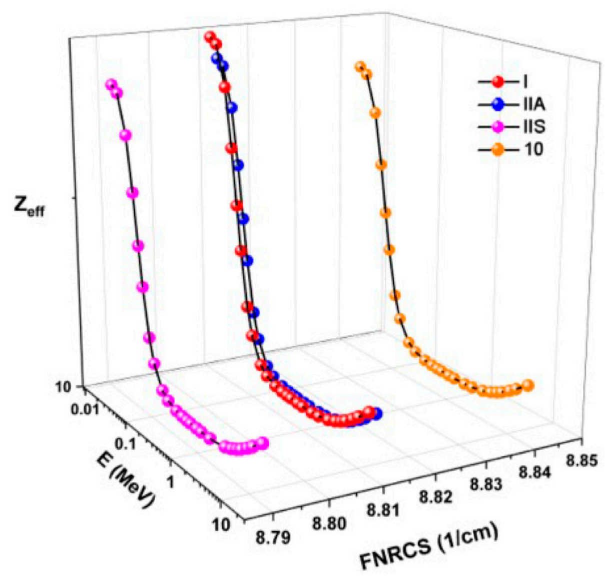

FIGURE 12
A three-dimensional plot illustrating the relationship between the effective atomic number (Zeff) and Fast neutron removal cross section (1/cm) as a function of energy for the Um Had granitoid.

Tables S2–S5) reveal an inverse relationship between the penetration depth and the incident photon energy. As the energy of the photons decreases, the depth-dependent absorbance increases, reaching its maximum in the medium energy range before starting to decline. This indicates that the granite rock samples (I, IIA, IIS, and 10) may offer better shielding for lower energy gamma rays but may lose effectiveness for higher energy gamma rays due to the decrease in depth-dependent absorbance.

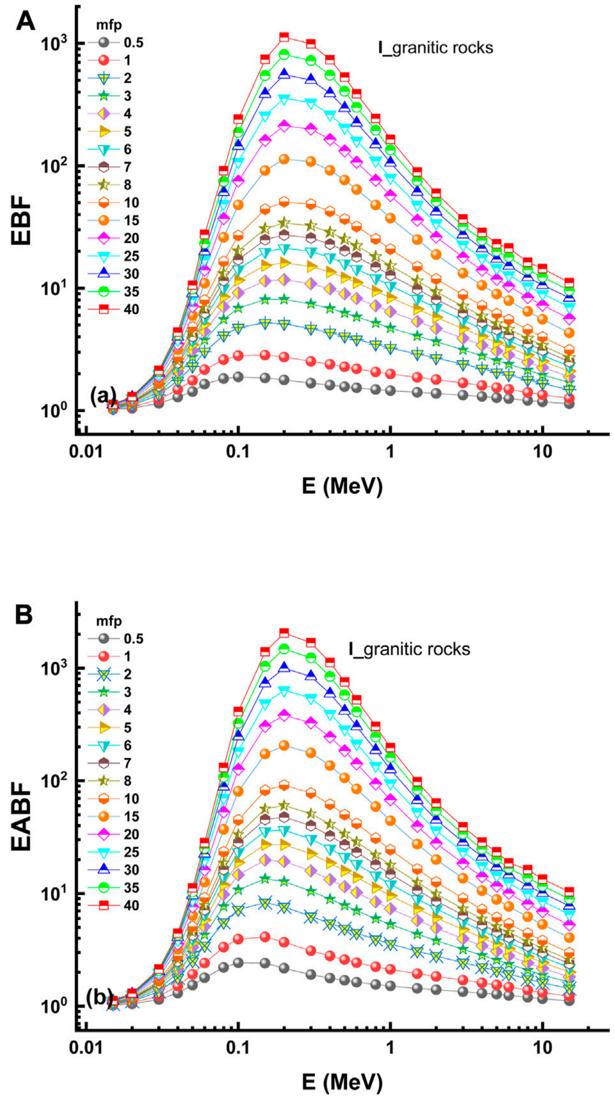

FIGURE 13
Illustration of the variation in: **(A)** exposure buildup factor (EBF) and **(B)** energy absorption buildup factor (EBF) in relation to photon energy in Um Had granitoid.

5 Conclusion

The present article studied the physico-mechanical characteristics and shielding efficiency of the Neoproterozoic granitoid of Um Had Area, Central Eastern Desert, Egypt with reference to their mineralogical and geochemical compositions. The main findings of this study are as follows:

- The studied granitoid rocks are characterized by their medium- to coarse-grained texture. They are classified as syenogranite based on their modal analyses and bulk rock chemistry.
- The main mineral composition of our studied granite samples includes quartz (22%-32%), microcline and orthoclase (35%-42%), and albite (8%-20%), in addition to minor amounts of biotite and hornblende. The predominant secondary minerals

are kaolinite, sericite and epidote while iron oxides and zircon represent the main accessory minerals.
- The physical test data revealed that the water absorption and bulk density are significantly influenced by the percentages of apparent porosity. The water absorption ranges from 0.38% to 0.55% with an average value of 0.41%. The bulk density ranges from 2559 to 2565 kg/m^3 with an average value of 2562 kg/m^3. At the same time, a negative variation in water absorption values is observed with the total normative feldspar content with a correlation coefficient of $r = -0.67$, while a positive variation with normative hematite content is observed with a correlation coefficient of $r = 0.77$.
- The mechanical properties of the studied granitoid rocks show that the compressive strength ranged from 509 to 1207 kg/cm^2 with an average value of 880 kg/cm^2. The results also exhibit a positive variation in compressive strength values with the normative albite content with a correlation coefficient ($r = 0.85$).
- The studied granitoid rocks satisfy the bulk density requirements of dimension stones and, to some extent, water absorption. Although the compressive strength values do not achieve the minimum requirements, they could be acceptable for interior use and light-duty purposes for exterior uses.
- This comprehensive analysis provides strong evidence of the granitoid capabilities as a radiation-shielding material. However, this study is but a small step forward in our understanding and application of geological samples for radiation protection.

Data availability statement

The datasets presented in this study can be found in online repositories. The names of the repository/repositories and accession number(s) can be found in the article/Supplementary Material.

Author contributions

Conceptualization, EL and MR; methodology, EL and MR; software, EL and MR; validation, EL, WA, MA, and MR formal analysis, WA, IT, and MR; investigation, EL and MR; resources, MA; data curation, EL, WA, MA, IT, MR, and HZ; writing—original draft preparation, EL, WA, MA, and MR; writing—review and editing, EL, SA, IT, AE, HZ, and MR; visualization, EL, IT, and MR; supervision, EL and MR; funding acquisition, SA, AE, and HZ. All authors contributed to the article and approved the submitted version.

Funding

This research was supported by the Researchers Supporting Project number (RSP2023R496), King Saud University, Riyadh, Saudi Arabia.

Acknowledgments

The authors greatly appreciate all efforts and supports offered by the “Marble and Granite Test Lab” unit (MGTL) and its members at the National Research Centre (NRC) for measuring all physical and mechanical properties of the collected rock samples, being the first pioneer, specialized, and accredited unit in the field of dimension and ornamental stones testing in Egypt. The authors also appreciate the help of XRF Lab for chemical analysis measurements. The author AE would like to thank “Dunarea de Jos” University of Galati, Romania, INPOLDE infrastructure, for the material and technical support.

Conflict of interest

The authors declare that the research was conducted in the absence of any commercial or financial relationships that could be construed as a potential conflict of interest.

Publisher’s note

Supplementary material

The Supplementary Material for this article can be found online at: https://www.frontiersin.org/articles/10.3389/feart.2023.1228489/full#supplementary-material

References

Abdel-Karim, A.-A., Azer, M., and Sami, M. (2021). Petrogenesis and tectonic implications of the maladob ring complex in the South Eastern Desert, Egypt: new insights from mineral chemistry and whole-rock geochemistry. *Int. J. Earth Sci.* 110, 53–80. doi:10.1007/s00531-020-01937-2

Abuamarah, B. A., Azer, M. K., Seddik, A. M. A., Asimow, P. D., Guzman, P., Fultz, B. T., et al. (2022). Magmatic and post-magmatic evolution of post-collisional rare-metal bearing granite: the neoproterozoic homrit akarem granitic intrusion, south Eastern Desert of Egypt, arabian-nubian Shield. *Geochemistry* 82, 125840. doi:10.1016/j.chemer.2021.125840

Alharshan, G. A., Kamar, M. S., Lasheen, E. S. R., Ene, A., Uosif, M. A. M., Awad, H. A., et al. (2022). Distribution of radionuclides and radiological health assessment in seih-sidri area, southwestern Sinai. *Int. J. Environ. Res. Public. Health* 19, 10717. doi:10.3390/ijerph191710717

Alzahrani, A. M., Lasheen, E. S. R., and Rashwan, M. A. (2022). Relationship of mineralogical composition to thermal expansion, spectral reflectance, and physico-mechanical aspects of commercial ornamental granitic rocks. *Materials* 15, 2041. doi:10.3390/ma15062041

ASTM C170/C170M (2015). *Standard test method for compressive strength of dimension stone*. West Conshohocken, PA (USA): American Society for Testing Materials.

ASTM C97/C97M (2015). *Standard test method for absorption and bulk specific gravity of dimension stone*. West Conshohocken: American Society for Testing Materials.

Azer, M. K., Abdelfadil, K. M., Asimow, P. D., and Khalil, A. E. (2020). Tracking the transition from subduction-related to post-collisional magmatism in the North arabian–nubian Shield: A case study from the homrit waggat area of the Eastern Desert of Egypt. *Geol. J.* 55, 4426–4452. doi:10.1002/gj.3643

EN, 1936. *European Standard Natural stone test method- Determination of apparent density and open porosity*. London: British Standard.

Ericsson, M. (2019). XXIX world marble and stones report 2018 by carlo montani: aldus casa di Edizioni, carrara Italy 2018 E-mail: aldus.danielecanal@alice.it. *Min. Econ.* 32, 255–256. doi:10.1007/s13563-019-00183-6

Eroğlu, G., and Çalik, A. (2023). Relationship of petrographic and mineralogical characteristics with mechanical strength properties of granitic rocks: A case study from the biga peninsula, NW Turkey. *Turk. J. Earth Sci.* doi:10.55730/1300-0985.1831

Fort, R., Alvarez de Buergo, M., Perez-Monserrat, E. M., Gomez-Heras, M., Jose Varas-Muriel, M., and Freire, D. M. (2013). Evolution in the use of natural building stone in Madrid, Spain. *Q. J. Eng. Geol. Hydrogeol.* 46, 421–429. doi:10.1144/qjegh2012-041

Gharib, M. G. (2012). Origin and evolution history of magmatic garnet-bearing pegmatites and associated granitoids, abu Had area, south Eastern Desert, Egypt: inference from petrology and geochemistry. *J. Am. Sci.* 8, 536–554.

Gomes, V. R., Babisk, M. P., Vieira, C. M. F., Sampaio, J. A., Vidal, F. W. H., and Gadioli, M. C. B. (2020). Ornamental stone wastes as an alternate raw material for soda-lime glass manufacturing. *Mat. Lett.* 269, 127579. doi:10.1016/j.matlet.2020.127579

Hamdy, M. M., Lasheen, E. S. R., and Abdelwahab, W. (2022). Gold-bearing listwaenites in ophiolitic ultramafics from the Eastern Desert of Egypt: subduction zone-related alteration of Neoproterozoic mantle? *J. Afr. Earth Sci.* 193, 104574. doi:10.1016/j.jafrearsci.2022.104574

Hassan, M. A., and Hashad, A. H. (1990). "Precambrian of Egypt," in *The geology of Egypt*. Editor R. Said (Rotterdam: Balkema), 201–245.

Kamar, M. S., Salem, I. A., El-Aassy, I. E., El-Sayed, A. A., Zakaly, H. M. H., Alzahrani, A. M., et al. (2022). An extended investigation of high-level natural radioactivity and geochemistry of neoproterozoic dokhan Volcanics: A case study of Wadi gebeiy, southwestern Sinai, Egypt. *Sustainability* 14, 9291. doi:10.3390/su14159291

Khaleal, F. M., El-Bialy, M. Z., Saleh, G. M., Lasheen, E. S. R., Kamar, M. S., Omar, M. M., et al. (2023a). Assessing environmental and radiological impacts and lithological mapping of beryl-bearing rocks in Egypt using high-resolution sentinel-2 remote sensing images. *Sci. Rep.* 13, 11497. doi:10.1038/s41598-023-38298-0

Khaleal, F. M., Lentz, D. R., Kamar, M. S., Saleh, G. M., and Lasheen, E. S. R. (2023b). Critical raw material resources in Nugrus-Sikait area, South Eastern Desert, Egypt: geological and geochemical aspects. *J. Afr. Earth Sci.* 197, 104782. doi:10.1016/j.jafrearsci.2022.104782

Khaleal, F. M., Saleh, G. M., Lasheen, E. S. R., Alzahrani, A. M., and Kamh, S. Z. (2022a). Exploration and petrogenesis of corundum-bearing pegmatites: A case study in migif-hafafit area, Egypt. *Front. Earth Sci.* 10, 869828. doi:10.3389/feart.2022.869828

Khaleal, F. M., Saleh, G. M., Lasheen, E. S. R., and Lentz, D. R. (2022b). Occurrences and genesis of emerald and other beryls mineralization in Egypt: A review. *Phys. Chem. Earth Parts ABC* 128, 103266. doi:10.1016/j.pce.2022.103266

Lasheen, E. S. R., Azer, M. K., Ene, A., Abdelwahab, W., Zakaly, H. M. H., Awad, H. A., et al. (2022a). Radiological hazards and natural radionuclide distribution in granitic rocks of homrit waggat area, central Eastern Desert, Egypt. *Materials* 15, 4069. doi:10.3390/ma15124069

Lasheen, E. S. R., Mohamed, W. H., Ene, A., Awad, H. A., and Azer, M. K. (2022b). Implementation of petrographical and aeromagnetic data to determine depth and structural trend of homrit waggat area, central Eastern Desert, Egypt. *Appl. Sci.* 12, 8782. doi:10.3390/app12178782

Lasheen, E. S. R., Rashwan, M. A., and Azer, M. K. (2023). Effect of mineralogical variations on physico-mechanical and thermal properties of granitic rocks. *Sci. Rep.* 13, 10320. doi:10.1038/s41598-023-36459-9

Lasheen, E. S. R., Saleh, G. M., Khaleal, F. M., and Alwetaishi, M. (2021). Petrogenesis of neoproterozoic ultramafic rocks, Wadi ibib–wadi shani, south Eastern Desert, Egypt: constraints from whole rock and mineral chemistry. *Appl. Sci. Switz.* 11, 10524. doi:10.3390/app112210524

Laurent, A., Janoušek, V., Magna, T., Schulmann, K., and Míková, J. (2014). Petrogenesis and geochronology of a post-orogenic calc-alkaline magmatic association: the žulová pluton, bohemian massif. *J. Geosci.*, 415–440. doi:10.3190/jgeosci.176

Madbouly, A. M., Sallam, O. I., Issa, S. A. M., Rashad, M., Hamdy, A., Tekin, H. O., et al. (2022). Experimental and FLUKA evaluation on structure and optical properties and γ-radiation shielding capacity of bismuth borophosphate glasses. *Prog. Nucl. Energy* 148, 104219. doi:10.1016/j.pnucene.2022.104219

Maniar, P. D., and Piccoli, P. M. (1989). Tectonic discrimination of granitoids. *Geol. Soc. Am. Bull.* 101, 635–643. doi:10.1130/0016-7606(1989)101<0635:TDOG>2.3

Mashaly, A. O., El-Kalioub y, B. A., Shalaby, B. N., El-Gohary, A. M., and Rashwan, M. A. (2016). Effects of marble sludge incorporation on the properties of cement composites and concrete paving blocks. *J. Clean. Prod.* 112, 731–741. doi:10.1016/j.jclepro.2015.07.023

Mashaly, A. O., Shalaby, B. N., and Rashwan, M. A. (2018). Performance of mortar and concrete incorporating granite sludge as cement replacement. *Constr. Build. Mat.* 169, 800–818. doi:10.1016/j.conbuildmat.2018.03.046

Middlemost, E. A. K. (1994). Naming materials in the magma/igneous rock system. *Earth-Sci. Rev.* 37, 215–224. doi:10.1016/0012-8252(94)90029-9

Mosch, S., and Siegesmund, S. (2007). Petrophysical and technical properties of dimensional stones: A statistical approach. *Z. Dtsch. Ges. Für Geowiss.* 158, 821–868. doi:10.1127/1860-1804/2007/0158-0821

Qaoud, N. (2014). Utilization of space-borne imagery for lithologic mapping: A case study from Um Had area, central Eastern Desert, Egypt. *J. Geogr. Geol.* 6, 113. doi:10.5539/jgg.v6n2p113

Rashwan, M. A., Al - Basiony, T. M., Mashaly, A. O., and Khalil, M. M. (2020). Behaviour of fresh and hardened concrete incorporating marble and granite sludge as cement replacement. *J. Build. Eng.* 32, 101697. doi:10.1016/j.jobe.2020.101697

Rashwan, M. A., Al Basiony, T. M., Mashaly, A. O., and Khalil, M. M. (2022). Self-compacting concrete between workability performance and engineering properties using natural stone wastes. *Constr. Build. Mat.* 319, 126132. doi:10.1016/j.conbuildmat.2021.126132

Rashwan, M. A., Lasheen, E. S. R., and Azer, M. K. (2023a). Thermal and physico-mechanical evaluation of some magmatic rocks at homrit waggat area, Eastern Desert, Egypt: petrography and geochemistry. *Bull. Eng. Geol. Environ.* 82, 199. doi:10.1007/s10064-023-03208-1

Rashwan, M. A., Lasheen, E. S. R., and Hegazy, A. A. (2023b). Tracking the pozzolanic activity of mafic rock powder on durability performance of cement pastes under adverse conditions: physico-mechanical properties, mineralogy, microstructure, and heat of hydration. *J. Build. Eng.* 71, 106485. doi:10.1016/j.jobe.2023.106485

Rashwan, M. A., Lasheen, E. S. R., and Shalaby, B. N. (2019). Incorporation of metagabbro as cement replacement in cement-based materials: A role of mafic minerals on the physico-mechanical and durability properties. *Constr. Build. Mat.* 210, 256–268. doi:10.1016/j.conbuildmat.2019.03.191

Rickwood, P. C. (1989). Boundary lines within petrologic diagrams which use oxides of major and minor elements. *Lithos* 22, 247–263. doi:10.1016/0024-4937(89)90028-5

Şakar, E., Özpolat, Ö. F., Alım, B., Sayyed, M. I., and Kurudirek, M. (2020). Phy-X/PSD: development of a user friendly online software for calculation of parameters relevant to radiation shielding and dosimetry. *Radiat. Phys. Chem.* 166, 108496. doi:10.1016/J.RADPHYSCHEM.2019.108496

Saleh, G. M., Kamar, M. S., Lasheen, E. S. R., Ibrahim, I. H., and Azer, M. K. (2022a). Whole rock and mineral chemistry of the rare metals-bearing mylonitic rocks, Abu Rusheid borehole, south Eastern Desert, Egypt. *J. Afr. Earth Sci.* 196, 104736. doi:10.1016/j.jafrearsci.2022.104736

Saleh, G. M., Khaleal, F. M., and Lasheen, E. S. R. (2022b). Geochemistry and paleoweathering of metasediments and pyrite-bearing quartzite during the neoproterozoic era, Wadi ibib-wadi suwawrib, south Eastern Desert, Egypt. *Arab. J. Geosci.* 15, 51. doi:10.1007/s12517-021-09141-5

Sami, M., Adam, M. M. A., Lv, X., Lasheen, E. S. R., Ene, A., Zakaly, H. M. H., et al. (2023). Petrogenesis and tectonic implications of the cryogenian I-type granodiorites from gabgaba terrane (NE Sudan). *Minerals* 13, 331. doi:10.3390/min13030331

Shand, S. J. (1951). *Eruptive rocks*. 4th edition. New York: John-Wiley.

S. Siegesmund and R. Snethlage (Editors) (2014). *Stone in architecture: Properties, durability* (Berlin, Heidelberg: Springer Berlin Heidelberg). doi:10.1007/978-3-642-45155-3

Singh, V. P., and Badiger, N. M. (2014). Energy absorption buildup factors, exposure buildup factors and Kerma for optically stimulated luminescence materials and their tissue equivalence for radiation dosimetry. *Radiat. Phys. Chem.* 104, 61–67. doi:10.1016/j.radphyschem.2013.11.025

Stern, R. J., and Hedge, C. E. (1985). Geochronologic and isotopic constraints on late Precambrian crustal evolution in the Eastern Desert of Egypt. *Am. J. Sci.* 285, 97–127. doi:10.2475/ajs.285.2.97

Streckeisen, A. (1976). To each plutonic rock its proper name. *Earth-Sci. Rev.* 12, 1–33. doi:10.1016/0012-8252(76)90052-0

Sun, S. -s., and McDonough, W. F. (1989). Chemical and isotopic systematics of oceanic basalts: implications for mantle composition and processes. *Geol. Soc. Lond. Spec. Publ.* 42, 313–345. doi:10.1144/GSL.SP.1989.042.01.19

Whalen, J. B., Currie, K. L., and Chappell, B. W. (1987). A-Type granites: geochemical characteristics, discrimination and petrogenesis. *Contrib. Mineral. Pet.* 95, 407–419. doi:10.1007/BF00402202

Whitney, D. L., and Evans, B. W. (2010). Abbreviations for names of rock-forming minerals. *Am. Mineral.* 95, 185–187. doi:10.2138/am.2010.3371